Progress In Electromagnetics Research B, Vol. 67, 17–30, 2016

Polarization Transformation by a Hyperbolic Metamaterial on a Metal Substrate

Illia Fedorin*

Abstract—In the present paper we focus on the study of polarization properties of biaxial metamaterial, which consist of alternate ferrite and semiconductor layers, located on an ideally conducted metal substrate. The system is placed into an external magnetic field along the boundaries of the layers. The effective medium theory is applied. Effective linear-to-elliptic polarization conversion has been shown, by means of physical and geometrical parameters of the system under consideration.

1. INTRODUCTION

Recently, a lot of investigations are pointed to the periodical structures that include layers made from natural or artificial materials with spatial dispersion. One-dimensional periodic structures have found particularly wide application as filters and lasers. They are the basis of distributed Bragg reflection lasers. Such structures realize the polarization transforming of waves in additional to their spatial and frequency selections. Note that in a one-dimensional case a photonic crystal (PC) is nothing more than a dielectric periodic layered structure. The PCs are now widely used in modern integrated optics and optoelectronics, laser and X-ray techniques, microwave and optical communications [1–5].

Electromagnetic properties of materials that have artificially created periodic translation symmetry are of great interest. There is a direct analogy between the wave processes in such structures and the properties of wave functions of electrons moving in the periodic potential of a crystal lattice. The translation symmetry significantly affects the spectrum of eigenwaves of such materials. There are alternating bandwidths in which propagation of electromagnetic waves is either allowed or forbidden [2, 6].

From the viewpoint of applications, it is obvious that not only the design of PCs but also the control of the position and width of the band gap and polarization state is of great interest. One of the ways to realize the control is using magnetic materials in the fabrication of PCs to produce so-called magnetophotonic crystals (MPCs). Indeed, a biased external static magnetic field can alter permittivity or permeability of MPC ingredients [2, 7].

From both fundamental and application points of view, the planar metamaterials placed on substrates of different natures, namely ferrite, dielectric, metallic, are quite interesting objects because they can be used successfully to design non-reciprocal magnetically controllable microwave devices. On the other hand, magneto-optically active substrate can serve as a sensitive element for THz magnetic near-field imaging in metamaterials. The polarization rotation of a near-IR probe beam revealed in the substrate measures the magnetic near-field [8]. Thus, the knowledge about optical properties of metamaterials based on the thin planar magnetic structures is especially important.

The research on effective control and manipulation of electromagnetic waves (EM) polarization states in PCs and metamaterials has been especially intense within microwaves. Polarization is one of

Received 17 January 2016, Accepted 26 March 2016, Scheduled 5 April 2016

* Corresponding author: Illia Fedorin (fedorin.ilya@gmail.com).

The author is with the Materials for Electronics and Solar Cells Department, National Technical University "Kharkiv Polytechnic Institute", Kharkiv, Ukraine.

the basic properties of electromagnetic waves conveying valuable information in signal transmission and sensitive measurements. Conventional methods for advanced polarization control impose demanding requirements on material properties and attain only limited performance. Conventional state-of-the-art polarization converters utilize birefringence or total internal reflection effects in crystals and polymers, which cause phase retardation between the two orthogonally polarized wave components [1].

Polarization conversion is important in many polarization-manipulating devices such as modulators, integrated switches, amplifiers, polarization splitters, and it has also been investigated theoretically using slightly different systems, such as a combination of anisotropic materials and corrugated surfaces, a dielectric-film waveguide with a corrugated cover layer, or a multilayered structure involving alternating birefringent biaxial layers. Nevertheless, with these techniques, perfect polarization conversion is difficult to achieve and the fabrication seems to be a demanding task [9].

Manipulation of wave polarization states is one of the essential and challenging tasks in the terahertz regime. Over the last few decades, various designs of polarizer's and wave plates have been proposed, including sheet polarizer's using anisotropic absorption media, prism polarizer's, Brewster-angle polarizer's, wire-grid polarizer's, as well as birefringence utilizing paper, liquid crystals, multi-layer meander liners and chiral effect. However, more convenient, and flexible approaches are always desirable to completely control the polarization states [10].

This has become possible with the advent of metamaterials that promise a variety of fascinating physical phenomena, such as negative refraction, invisibility cloaking, superfocusing and miniaturized antennas [10–17].

A number of papers are devoted to the solution of mentioned problems. For example, it has been demonstrated in [1], ultrathin, broadband, and highly efficient metamaterial-based terahertz polarization converters are capable of rotating a linear polarization state into its orthogonal one, and the prototype structures capable of realizing nearperfect anomalous refraction. In [2], the polarization properties of a magnetophotonic layered structure were studied at the frequencies close to the frequency of ferromagnetic resonance. The investigations were carried out taking into account a great value of dissipative losses in biased ferrite layers in this frequency band. In [12], the scattering and TE/TM polarization conversion characteristics of LH-grating in the case of plane wave oblique incidence were analyzed, and comparison between RH-gratings and LH-gratings was given with physical explanations. In [8], the spectral and polarization properties of electromagnetic wave through a planar chiral structure, loaded with the gyrotropic medium under an action of the longitudinal magnetic field, was studied. In [14], the approaches for determining the eigenpolarizations in an arbitrary diffraction order of any planar periodic structure (PPS) under arbitrary incidence has been proposed. In [15], a homogeneous circular polarizer based on a bilayered chiral metamaterial with two enantiomeric wheel patterns was proposed. The authors in [16] experimentally investigated the rotation of polarization plane of electromagnetic waves by the metallic helices. The polarization properties of perfectly periodical and defective one-dimensional photonic band gap structures with nonreciprocal chiral (bi-isotropic) layers were studied in [5]. The reflection, transmission spectra and the polarization transformation of linearly polarized waves in the ferrite-semiconductor multilayer structure were considered in [18]. In the long-wavelength limit, the effective medium theory is applied to describe the studied structure as a uniaxial anisotropic homogeneous medium defined by effective permittivity and effective permeability tensors. The authors in [10] show that a specially designed planar metamaterial can be employed to manipulate the polarization state of terahertz waves. By altering the geometric parameters of the metamaterial unit cells, we experimentally and numerically demonstrate that the polarization of the incident linearly polarized terahertz waves can be effectively converted. In our recent papers [19, 20], polarization conversion by a 1-d photonic crystal, which consists of alternating semiconductor and dielectric layers, located on isotropic and anisotropic substrates was considered.

Metamaterials have enabled the realization of many phenomena and functionalities unavailable using natural materials. Many basic metamaterial structures, such as metal split-ring resonators, exhibit birefringence suitable for polarization conversion, which has been mostly investigated in the microwave frequency range. Broadband metamaterial circular polarizers have been demonstrated in the optical regime using gold helix structures, and stacked nano-rod arrays with a tailored rotational twist. Metamaterial based polarimetric devices are particularly attractive in the terahertz (THz) frequency range due to the lack of suitable natural materials for THz device applications. However, the currently

available designs suffer from either very limited bandwidth or high losses [1, 11, 21, 22].

With the aim to further clarify the interesting properties of metamaterials, in the present paper we focus on the study of polarization properties of biaxial metamaterial on the metal substrate, which is composed of periodically alternating semiconductor and ferrite layers and is placed into an external magnetic field, parallel to the boundaries of the layers. The characteristic ranges near hybrid frequency in semiconductor and frequency of ferromagnetic resonance in the ferrite layer are considered precisely. The influence of dissipations is numerically investigated.

2. GEOMETRY OF THE STRUCTURE BASIC EQUATIONS

Let us analyze the polarization properties of the TE and TM arbitrary incident plane-wave by a magnetoactive subwavelength metamaterial in an external magnetic field, which is placed on the ideally conducting metal substrate. Consider a finite multilayered periodic structure, where the ferrite layers of thickness d_1 and the semiconductor layers of thickness d_2 alternate (Fig. 1). Assume that the thickness of the structure is L ($L = Nd$, where $N$is the number of periods, and $d = d_1 + d_2$ is the period of the structure). Let the structure be placed into an external magnetic field H_0 along y axis (parallel to the boundaries of the layers). The z axis runs perpendicularly to the boundaries of the layers (periodicity axis). The incident, reflected and transmitted wave vectors lie in the xz plane. In this case, we can put $\partial/\partial y = 0$, omitting the dependence on the coordinate y in the equations.

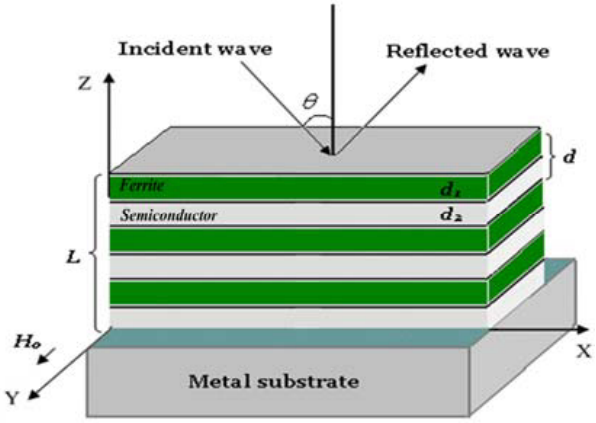

Figure 1. Geometry of the structure.

For the chosen geometry of the structure, the Maxwell's equations can be separated into the equations for two modes with different polarizations. To analyze the polarization properties, we consider both the TE-polarization with components H_x, H_z, E_y (ordinary waves) and TM-polarization with components E_x, E_z, H_y (extraordinary waves).

To solve the problem, we use Maxwell equations in the ferrite and semiconductor layers, the equations of continuity and the motion of charge carries. We seek the variables in these equations in the form of $\exp[ik_x x + ik_z z - i\omega t]$. We also apply boundary conditions for the tangential field components at the layers interfaces.

The dispersion equation for TM-waves in the infinite periodic structure, which relates the frequency ω and the Bloch wave number $\overline{k}^{TM}$, can be written as [23, 24]

$$\begin{aligned}\cos \bar{k}^{TM} d \;=\; & \cos k_{z1}^{TM} d_1 \cos k_{z2}^{TM} d_2 \\ & -\frac{\varepsilon_f^s \varepsilon_F}{2k_{z1}^{TM} k_{z2}^{TM}} \left(\left(\frac{k_{z1}^{TM}}{\varepsilon_F} \right)^2 + \left(\frac{k_{z2}^{TM}}{\varepsilon_f^s} \right)^2 - \left(\frac{k_x}{\varepsilon_f^s} \frac{\varepsilon_\perp}{\varepsilon_\parallel} \right)^2 \right) \sin k_{z1}^{TM} d_1 \sin k_{z2}^{TM} d_2 \end{aligned} \tag{1}$$

where $k_{z1}^{TM} = \sqrt{(\omega/c)^2 \varepsilon_F - k_x^2}$ and $k_{z2}^{TM} = \sqrt{(\omega/c)^2 \varepsilon_f^s - k_x^2}$ are the transversal wave numbers of

ferrite and semiconductor layers for TM-waves, respectively; k_x is the longitudinal wave number; ε_F is permittivity of the ferrite layer; $\varepsilon_f^s = \varepsilon_\parallel + \varepsilon_\perp/\varepsilon_\parallel$ is the Voigt effective permittivity of the semiconductor layer; $\varepsilon_\parallel$ and $\varepsilon_\perp$ are the components of semiconductor permittivity tensor, which for the investigated THz region can be given as [6, 23]

$$\varepsilon_s = \begin{pmatrix} \varepsilon_{xx} & 0 & \varepsilon_{xz} \\ 0 & \varepsilon_{yy} & 0 \\ \varepsilon_{zx} & 0 & \varepsilon_{zz} \end{pmatrix},$$

where

$$\begin{aligned} \left(\varepsilon_{xx}^s\right) &= \left(\varepsilon_{zz}^s\right) = \varepsilon_\parallel = \varepsilon_0 \left(1 - \frac{\omega_P^2 (\omega + i\upsilon)}{\omega \left[(\omega + i\upsilon)^2 - \omega_C^2\right]}\right), \\ \left(\varepsilon_{xz}^s\right) &= -\left(\varepsilon_{zx}^s\right) = \varepsilon_\perp = -i\varepsilon_0 \left(\frac{\omega_P^2 \omega_C}{\omega \left[(\omega + i\upsilon)^2 - \omega_C^2\right]}\right), \\ \left(\varepsilon_{yy}^s\right) &= \varepsilon_0 \left(1 - \frac{\omega_P^2}{\omega (\omega + i\upsilon)}\right). \end{aligned}$$

Here ε_0 is the part of the permittivity attributed to the lattice; $\omega_p = \sqrt{4\pi e^2 n_0 / m_{eff} \varepsilon_0}$ is the plasma frequency; $\omega_C = eH_0/m_{eff}c$ is the cyclotron frequency; υ is the electron collision frequency; e, n_0, and m_{eff} are the charge, concentration, and effective mass of charge carriers. The permeability for nonmagnetic semiconductor layer is $\mu^s = 1$.

Similarly, the dispersion equation for TE-waves in the infinite periodic structure can be written as [7, 25]

$$\cos \bar{k}^{TE} d = \cos k_{z1}^{TE} d_1 \cos k_{z2}^{TE} d_2 - \frac{\mu_F}{2 k_{z1}^{TE} k_{z2}^{TE}} \left[\left(\frac{k_{z1}^{TE}}{\mu_F}\right)^2 + \left(k_{z2}^{TE}\right)^2 - \left(\frac{k_x \mu_\perp}{\mu_\parallel \mu_F}\right)^2\right] \sin k_{z1}^{TE} d_1 \sin k_{z2}^{TE} d_2, \tag{2}$$

where $k_{z1}^{TE} = \sqrt{\left(\frac{\omega}{c}\right)^2 \mu_F \varepsilon_F - k_x^2}$, $k_{z2}^{TE} = \sqrt{\left(\frac{\omega}{c}\right)^2 \left(\varepsilon_{yy}^s\right) - k_x^2}$ are the transverse wave numbers of the ferrite and semiconductor layers for TE-waves, respectively; $\mu_F = \mu_\parallel + \frac{\mu_\perp^2}{\mu_\parallel}$ is the effective permeability; $\mu_\parallel = \mu_{xx} = \mu_{zz} = 1 + \frac{\omega_M \left(\omega_H^2 + \omega_r^2 - i\omega\omega_r\right)}{\omega_H \left(\omega_H^2 + \omega_r^2 - \omega^2 - 2i\omega\omega_r\right)}$, $\mu_\perp = \mu_{xz} = -\mu_{zx} = -\frac{i\omega\omega_M}{\omega_H^2 + \omega_r^2 - \omega^2 - 2i\omega\omega_r}$ are the components of the ferrite permeability tensor; $\omega_M = 2\pi e g M/mc$; $\omega_H = egH_0/2mc$; g is the factor of spectroscopic splitting; M is the saturation magnetization; ω_r is the relaxation frequency; $m$is electron free mass.

It should be noted that we applied the "resonant model" of the "saturated" ferrite to calculate the ferrite constitutive parameters, in the case when the static magnetic field H_0 is stronger than the field of the saturation magnetization $4\pi M$.

When static magnetic field is quite small, the "non-resonant" model of "non-saturated" ferrite should be applied. In this case, the current magnetization M is a function of the static magnetic field [8].

Moreover, in the considered geometry, the external magnetic field affects the TE-wave properties in a ferrite layer only (as ferrite transversal wavenumber k_{z1}^{TE} includes effective permeability μ_F, which is magnetic field dependent, whereas semiconductor transversal wavenumber k_{z2}^{TE} is magnetic field independent), and the TM-wave properties in a semiconductor layer only (as ferrite transversal wavenumber k_{z1}^{TM} is magnetic field independent, whereas semiconductor transversal wavenumber k_{z2}^{TM} includes Voigt effective permittivity ε_f^s, which is magnetic field dependent).

Let us consider dispersion Equations (1) and (2) in the subwavelength approximation regime, that is when $k_{z1}^{TE,TM} d_1$, $k_{z2}^{TE,TM} d_2$, $\bar{k}^{TE,TM} d << 1$. Physically it means that the period of the multilayer magnetoactive periodic structure is much less than the wavelength along z axis ($d << \lambda$). In this case,

the Bloch wave numbers $\bar{k}^{TM,TE} = k_z^{TM,TE}$ are the effective transverse wave numbers of a bigyrotropic metamaterial [7, 23, 25]

$$k_z^{TE} = \sqrt{\left(\frac{\omega}{c}\right)^2 \mu_{xx}\varepsilon_{yy} - \frac{\mu_{xx}}{\mu_{zz}}k_x^2}, \quad k_z^{TM} = \sqrt{\left(\frac{\omega}{c}\right)^2 \varepsilon_{xx} - \frac{\varepsilon_{xx}}{\varepsilon_{zz}}k_x^2}. \tag{3}$$

Here μ_{xx},μ_{zz} and ε_{xx}, ε_{yy}, ε_{zz} are the components of the effective permeability and permittivity tensors, respectively:

$$\begin{array}{l} \varepsilon_{xx} = \dfrac{\varepsilon_F d_1 + \varepsilon_f d_2}{d},\ \varepsilon_{yy} = \dfrac{\varepsilon_F d_1 + \left(\varepsilon_{yy}^s\right) d_2}{d}, \\ \varepsilon_{zz} = \dfrac{\varepsilon_{xx} d^2}{d_1 d_2 \left(\varepsilon_f/\varepsilon_F + \varepsilon_F/\varepsilon_\parallel\right) + d_1^2 + d_2^2}, \end{array} \quad , \quad \varepsilon^{eff} = \begin{pmatrix} \varepsilon_{xx} & 0 & 0 \\ 0 & \varepsilon_{yy} & 0 \\ 0 & 0 & \varepsilon_{zz} \end{pmatrix}. \tag{4}$$

$$\begin{array}{l} \mu_{xx} = \dfrac{\mu_f d_1 + d_2}{d},\ \mu_{zz} = \dfrac{\mu_{xx}\mu_{zz}^*}{\mu_{xx} + \alpha\mu_{zz}^*}, \\ \mu_{zz}^* = \dfrac{d\mu_f}{\mu_f d_2 + d_1}, \alpha = \dfrac{d_1 d_2}{d^2 \mu_f}\left(\dfrac{\mu_\perp}{\mu_\parallel}\right)^2, \end{array} \quad , \quad \mu^{eff} = \begin{pmatrix} \mu_{xx} & 0 & 0 \\ 0 & 1 & 0 \\ 0 & 0 & \mu_{zz} \end{pmatrix}. \tag{5}$$

The Maxwell equations for the considered metamaterial, with the effective permittivity and permeability tensors in Eqs. (4) and (5), can be generally split into the following equations for TM and TE polarizations:

$$\begin{cases} \dfrac{\partial E_y}{\partial z} + \dfrac{i\omega}{c}\mu_{xx}H_x = 0 \\ \dfrac{\partial E_y}{\partial x} - \dfrac{i\omega}{c}\mu_{zz}H_z = 0 \\ \dfrac{\partial H_x}{\partial z} - \dfrac{\partial H_z}{\partial x} + \dfrac{i\omega}{c}\varepsilon_{yy}E_y = 0 \end{cases}, \quad \begin{cases} \dfrac{\partial E_x}{\partial z} - \dfrac{\partial E_z}{\partial x} - \dfrac{i\omega}{c}H_y = 0 \\ \dfrac{\partial H_y}{\partial z} - \dfrac{i\omega}{c}\varepsilon_{xx}E_x = 0 \\ \dfrac{\partial H_y}{\partial x} + \dfrac{i\omega}{c}\varepsilon_{zz}E_z = 0 \end{cases}. \tag{6}$$

The electrodynamics properties of the anisotropic structure depend heavily on the direction of the wave propagation. The presence of a constant magnetic field brings about a number of specific features in the interaction of waves.

Thus, the considered structure in the long wave approximation can be described using effective medium theory, and it is possible to introduce effective permeability and permittivity tensors components to describe the electrodynamics properties. As can be seen, the components of permeability and permittivity depend heavily on the frequency, external magnetic field and physical and geometrical parameters of the constitutive layers. The analysis of the TE polarization wave spectral properties has been done in [7, 25]. So here we focus only on the specific features that are essential to the given work including analysis of TM polarization waves.

Let us analyze the frequency and external magnetic field dependence of effective components of permittivity, permeability, and Bloch wave numbers. The detailed analysis of expression for permeability of ferrite layer and permittivity of semiconductor layer can be found for example in [7, 25] and [6, 23], respectively. In order to be in accordance with the existent theoretical and experimental works [7] and [25], let us use the same numerical values of parameters. The ferrite layers (brand 1SCH4, the polycrystalline nickel ferrite NiO Fe_2O_3) have the following parameters $\varepsilon_F = 11.1$, $g = 2$, $d_1 = 0.05\,\text{cm}$, and saturation magnetization $M = 4800G$. The semiconductor layer (n-InSb) has parameters $\varepsilon_f = 17.8$, $d_1 = 0.05$ cm, $\omega_p = 2 \cdot 10^{12}\,\text{s}^{-1}$. We ignore the collision frequency in the semiconductor layers and magnetic damping in the ferrite, that is $\nu = 0$, and $\omega_r = 0$.

As can be easily seen (Fig. 2, and Fig. 3), there are a number of specific features at the corresponding dependencies, which correspond to the frequencies and magnetic fields where the components of effective permittivities and permeabilities tend to zero or infinity (it should be noted hereinafter that in the real material condition, when the dissipation processes are taken into account, the corresponding dependencies are smoothed, and there are, in fact, no infinity values, and near zero values occur).

Thus, at frequency $\omega_{\mu xz0} = \sqrt{(\omega_H + \omega_M)\left(\omega_H + \omega_H \frac{d_f}{d_f + d_s}\right)}$ and at the corresponding magnetic field $H_{\mu xz0}$, both μ_{xx} and μ_{zz} components of effective permeability tend to zero (Fig. 2). At the frequency of

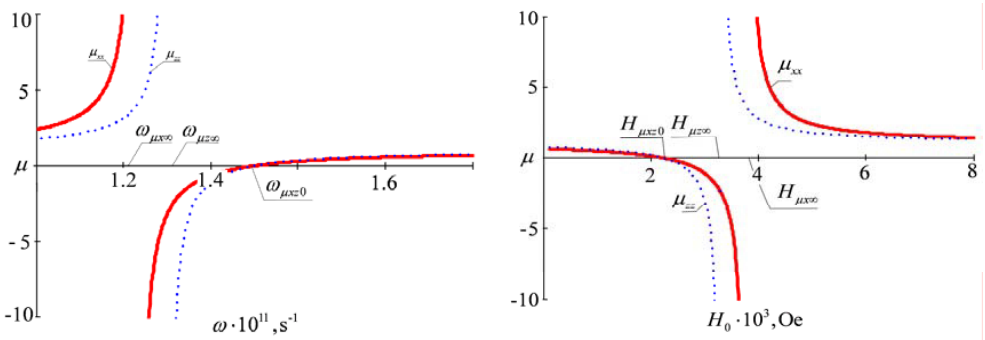

Figure 2. Permeability as a function of frequency (at constant magnetic field $H_0 = 5000\,\mathrm{Oe}$) and external magnetic field (at constant frequency $\omega = 10^{11}\,\mathrm{s}^{-1}$).

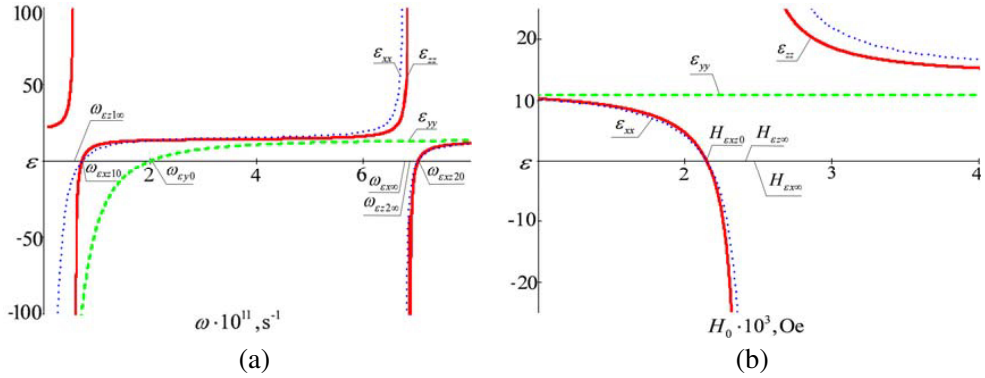

Figure 3. Permittivity as a function of frequency (at constant magnetic field $H_0 = 5000\,\mathrm{Oe}$) and external magnetic field (at constant frequency $\omega = 4 \cdot 10^{12}\,\mathrm{s}^{-1}$).

ferromagnetic resonance $\omega_{\mu x\infty} = \sqrt{\omega_H\left(\omega_H + \omega_M\right)}$ and at corresponding magnetic field $H_{\mu x\infty}$, the μ_{xx} components of effective permeability of metamaterial and effective permeability of ferrite layer μ_F tend to infinity (here $\mu_{\|} \to 0$). It can also be noted that at frequency $\omega = \omega_H$ parallel component of ferrite permeability ($\mu_{\|}$) and imaginary part of perpendicular component ($\mu_{\perp}$) tend to infinity. At frequency of anti-ferromagnetic resonance $\omega_{af} = (\omega_H + \omega_M)$ and at the corresponding magnetic field, the effective permeability of ferrite layer becomes zero $\mu_F \to 0$. Finally, at magnetic field $H_{\mu z\infty}$ and at frequency $\omega_{\mu z\infty}$, the μ_{zz} component of effective permeability tends to infinity.

A similar situation takes place at the effective permittivity dependence as a function of frequency and magnetic field (Fig. 3). Thus, at hybrid frequency $\omega_{\varepsilon x\infty} = \sqrt{\omega_C^2 + \omega_P^2}$ and corresponding magnetic field $H_{\varepsilon x\infty} = (m_{eff}c/e)\sqrt{\omega^2 - \omega_p^2}$, the parallel component of effective permittivity of metamaterial, and Voigt effective permittivity of semiconductor layer tend to infinity ($\varepsilon_{xx}, \varepsilon_f^s \to \infty$). At frequency $\omega_{\varepsilon y0} = \sqrt{\frac{\omega_P^2 \varepsilon_0 d_s}{\varepsilon_0 d_s + \varepsilon_f d_f}}$, the ε_{yy} component of effective permittivity tends to zero. At cyclotron frequency $\omega = \omega_C$, the permittivity semiconductor components $\varepsilon_{\perp}$ and $\varepsilon_{||}$ tend to infinity. At plasma frequency $\omega = \omega_P$, the ε_{yy}^s component of semiconductor permittivity tensor tends to infinity. At frequency $\omega_{\varepsilon xz10,\varepsilon xz20} = \sqrt{\left(a_2 \pm \sqrt{a_2^2 - 4a_1a_3}\right)\Big/ 2 \cdot a_1}$ ($a_1 = d_s\varepsilon_0 + d_f\varepsilon_f^s$, $a_2 = \omega_C^2 a_1 + \omega^2\left(d_s\varepsilon_0 + a_1\right)$, $a_3 = d_s\varepsilon_0\omega_p^4$) and at the corresponding magnetic field $H_{\varepsilon xz0}$, both ε_{xx} and ε_{zz} components of effective permittivity tend to zero. Finally, at magnetic field $H_{\varepsilon z\infty}$ and at frequency $\omega_{\varepsilon z1\infty,\varepsilon z2\infty}$, the ε_{zz} component of effective permittivity tends to infinity.

Table 1. Effective permeability behavior.

	Negative	Positive
μ_{xx}	$\omega_{\mu x\infty} < \omega < \omega_{\mu xz0}$ $H_{\mu xz0} < H_0 < H_{\mu x\infty}$	$\omega < \omega_{\mu x\infty}; \omega > \omega_{\mu xz0}$ $H_0 < H_{\mu xz0}; H_0 > H_{\mu x\infty}$
μ_{zz}	$\omega_{\mu z\infty} < \omega < \omega_{\mu xz0}$ $H_{\mu xz0} < H_0 < H_{\mu z\infty}$	$\omega < \omega_{\mu z\infty}; \omega > \omega_{\mu xz0}$ $H_0 < H_{\mu xz0}; H_0 > H_{\mu z\infty}$

Table 2. Effective permittivity behavior.

	Negative	Positive
ε_{xx}	$\omega < \omega_{\varepsilon xz10}; \omega_{\varepsilon x\infty} < \omega < \omega_{\varepsilon xz20}$ $H_{\varepsilon xz0} < H_0 < H_{\varepsilon x\infty}$	$\omega_{\varepsilon xz10} < \omega < \omega_{\varepsilon x\infty}; \omega > \omega_{\varepsilon xz20}$ $H_0 < H_{\varepsilon xz0}; H_0 > H_{\varepsilon x\infty}$
ε_{yy}	$\omega < \omega_{\varepsilon y0}$	$\omega > \omega_{\varepsilon y0}$
ε_{zz}	$\omega_{\varepsilon z1\infty} < \omega < \omega_{\varepsilon xz10}; \omega_{\varepsilon z2\infty} < \omega < \omega_{\varepsilon xz20}$ $H_{\varepsilon xz0} < H_0 < H_{\varepsilon z\infty}$	$\omega < \omega_{\varepsilon z1\infty}; \omega_{\varepsilon xz10} < \omega < \omega_{\varepsilon z2\infty}; \omega > \omega_{\varepsilon xz20}$ $H_0 < H_{\varepsilon xz0}; H_0 > H_{\varepsilon z\infty}$

We can sum up all previous analysis in the following tables, which show the regions where the components of effective permittivity and permeability become negative.

As we can see, there exist a number of regions where the components of permittivity and permeability become negative or positive. This behavior results in specific physical properties of such metamaterials in the corresponding regions. Thus, for example, in the frequency range $\omega_{\mu z\infty} < \omega < \omega_{\mu xz0}$, there are simultaneously negative μ_{xx} and μ_{zz} components of effective permeability. Moreover, at the used material parameters, in the mentioned frequency range, ε_{yy} component of effective permittivity is also negative (it should be noted that these ranges may differ depending on the plasma frequency value, external magnetic field value, and other physical parameters of materials that used). Thus, in this frequency range, the metamaterial, optically, behaves as a left-handed metamaterial for TM-polarized waves. By varying the material parameters, such as thicknesses of the layers, physical parameters of materials, etc., it is possible to effectively control the corresponding properties in the considered structure. However, when the dissipations are taken into account, the corresponding features are smoothed, and a highly precise control is necessary to support this conditions.

The frequency ranges, where the components $\mu_{xx} - \mu_{zz}$ and $\varepsilon_{xx} - \varepsilon_{zz}$ have opposite signs, relate to the so called hyperbolic metamaterials which are one of the most unusual classes of electromagnetic metamaterials. They display hyperbolic (or indefinite) dispersion, which originates from one of the principal components of their electric or magnetic effective tensor having the opposite sign to the other two principal components. Such anisotropic structured materials exhibit distinctive properties, including strong enhancement of spontaneous emission, diverging density of states, negative refraction and enhanced superlensing effects [11].

These regions are of great interest because of unusual properties of structures in such conditions. A number of interesting effects arise at mentioned characteristic frequencies and magnetic fields from the view point of current study of polarization properties of metamaterial placed on a metal substrate. This is described in the following sections.

As for dependencies of Bloch's wave numbers of the metamaterial as a function of external magnetic field and frequency (Figs. 4 and 5), they are in strong accordance with physical properties of effective components of permittivity and permeability. Namely, there are a number of characteristic points where Bloch's wave numbers become zero or tend to infinity and hence, become pure real or pure imaginary (it is possible only when dissipation is neglected, and in the real conditions, Bloch's wave numbers are complex). It means that these characteristic features influence the existence of allowed and forbidden zones of the metamaterial.

Thus, at frequencies $\omega_{\mu x\infty}$ and the corresponding magnetic fields $H_{\mu x\infty}$, the transversal effective

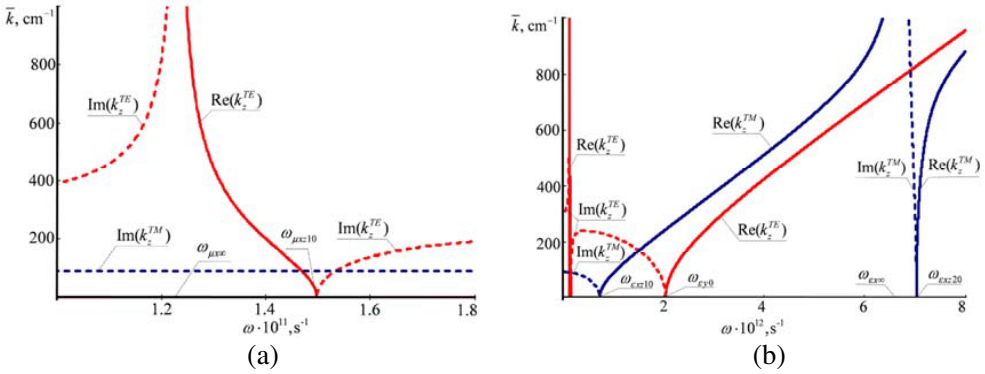

Figure 4. Bloch's wave numbers of the metamaterial as a function of frequency ($H_0 = 5000\,\mathrm{Oe}$).

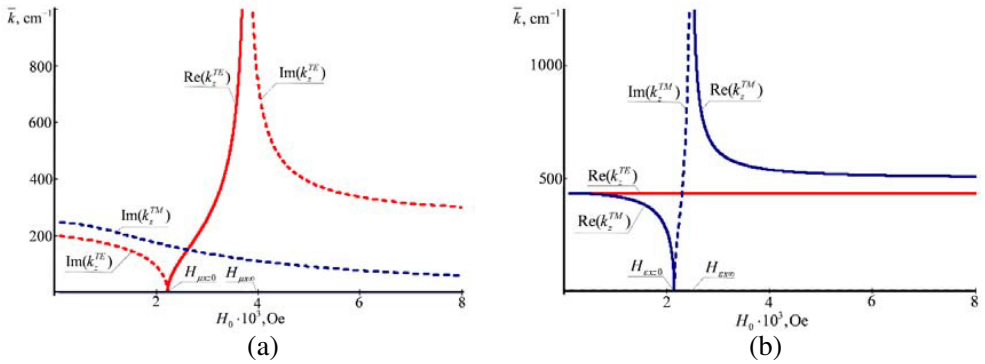

Figure 5. Bloch's wave numbers of the metamaterial as a function of external magnetic field for different frequencies: (a) $\omega = 10^{11}\,\mathrm{s}^{-1}$; (b) $\omega = 4\cdot10^{12}\,\mathrm{s}^{-1}$.

wave number for TE waves tends to infinity $k_z^{TE} \to \infty$; similarly, at the frequency $\omega_{\varepsilon x\infty}$ and magnetic field $H_{\varepsilon x\infty}$, the transversal effective wave number for TM waves tends to infinity $k_z^{TM} \to \infty$. At frequencies $\omega_{\varepsilon xz10,\varepsilon xz20}$ and magnetic field $H_{\varepsilon xz0}$, $k_z^{TM} \to 0$. On the other hand, at frequencies $\omega_{\mu xz0}$, $\omega_{\varepsilon y0}$ and magnetic field $H_{\mu xz0}$, $k_z^{TE} \to 0$.

To summarize the above results, we can effectively control the band structure of the effective metamaterial by means of frequency, external magnetic field, and other physical and geometrical parameters of the materials that form the structure. Both single-mode (TE or TM) and multimode regime can be supported under the corresponding parameters of the metamaterial.

3. THEORETICAL ANALYSIS

Let us now assume that the structure located on an ideally conducting metal substrate. This geometry is very useful from the view point of practical application as thin-films on the ideally conducting substrates are widely used in optics and electronics.

It is well known that in this case, the tangential components of electric field and normal component of magnetic field should be equal 0 at the metal boundary, that is $E_t = 0, H_n = 0$ [26]. Using the boundary conditions, it is easy to derive the equations for reflection and transmission coefficients for the system under consideration

$$\begin{aligned} A^{TE} &= \frac{-e^{2ik_z^{TE}L}\left(k_z^{TE} + k_{zv}\mu_{xx}\right) + \left(k_{zv}\mu_{xx} - k_z^{TE}\right)}{-e^{2ik_z^{TE}L}\left(k_{zv}\mu_{xx} - k_z^{TE}\right) + \left(k_{zv}\mu_{xx} + k_z^{TE}\right)}, \\ A^{TM} &= \frac{e^{-2ik_z^{TM}L}\left(k_{zv}\varepsilon_{xx} - k_z^{TM}\varepsilon_v\right) + \left(k_{zv}\varepsilon_{xx} + k_z^{TM}\varepsilon_v\right)}{e^{-2ik_z^{TM}L}\left(k_{zv}\varepsilon_{xx} + k_z^{TM}\varepsilon_v\right) + \left(k_{zv}\varepsilon_{xx} - k_z^{TM}\varepsilon_v\right)}. \end{aligned} \tag{7}$$

Then the phase constants for TE and TM polarized waves can be written as

$$\begin{aligned}\delta^{TM} &= \arg A^{TM} = 2arctg\left[\frac{k_z^{TM}\varepsilon_v}{k_{zv}\varepsilon_{xx}}tgk_z^{TM}L\right],\\ \delta^{TE} &= \arg A^{TE} = -2arctg\left[\frac{k_z^{TE}}{k_{zv}\mu_{xx}}ctgk_z^{TE}L\right].\end{aligned} \tag{8}$$

The phase difference $\delta = \delta^{TM} - \delta^{TE}$ can be calculated as follows:

$$\delta = 2\left(\text{arctg}\left[\frac{k_z^{TM}\varepsilon_v}{k_{zv}\varepsilon_{xx}}\text{tg}k_z^{TM}L\right] + \text{arctg}\left[\frac{k_z^{TE}}{k_{zv}\mu_{xx}}\text{ctg}k_z^{TE}L\right]\right). \tag{9}$$

Let us analyze the phase change at electromagnetic waves reflection from the metamaterial on the metal substrate.

Let's analytically consider the obtained expressions for δ^{TM} and δ^{TE}.

TM-polarized waves:

— $\delta^{TM} = 0$ when the Bloch wave number for TM-waves of the bigyrotropic metamaterial is equal to zero ($k_z^{TM} = 0$), and then $\text{tg}k_z^{TM}L = 0$; this occurs at $L = n\frac{\lambda^{TM}}{2}$, when $n = 0, 1, 2, \ldots$. Thus, the TM wave phase constant δ^{TM} becomes zero when the thickness of the structure is equal to the integer number of half wavelength (in the case of so-called Bragg resonance). It can also be shown that this condition is satisfied at the following incident angles:

$$\theta_{0TM} = \arcsin\sqrt{\varepsilon_{zz}\left(1 - \frac{n^2c^2\pi^2}{\omega^2L^2\varepsilon_{xx}}\right)},\ n = 0, 1, 2, \ldots$$

— $\delta^{TM} = 0$, if $\varepsilon_{xx} \to \infty$. Near this characteristic area (hybrid frequency or corresponding external magnetic field value), there is a large number of closely located zones of phase difference fast changes. This is due to the large values of k_z^{TM}.

— $\delta^{TM} = \pm\pi$, at $\text{tg}k_z^{TM}L \to \infty$, that is when $L = n\frac{\lambda^{TM}}{4}$, where $n = 1, 3, 5, \ldots$. So this condition takes place when the thickness of the structure is equal to the quarter wavelength or at the following incident angles

$$\theta_{\pm\pi TM} = \arcsin\sqrt{\varepsilon_{zz}\left(1 - \frac{n^2c^2\pi^2}{4\omega^2L^2\varepsilon_{xx}}\right)},\ n = 1, 3, 5, \ldots;$$

— $\delta^{TM} = \pm\pi$, when $\varepsilon_{xx} = \varepsilon_{zz} = 0$;

— at $L = n\frac{\lambda^{TM}}{8} \Rightarrow \text{tg}k_z^{TM}L = \pm 1$. Here the upper sign corresponds to $n = 1, 5, 9...$, and the lower sign to $n = 3, 7, 11, \ldots$. When this condition takes place, the phase of TM waves can be determined as follows:

$$\delta^{TM} = 2\text{arctg}\left[\frac{\pm k_z^{TM}\varepsilon_v}{k_{zv}\varepsilon_{xx}}\right].$$

Analogously for TE polarized wave:

— $\delta^{TE} = 0$, when $\text{ctg}k_z^{TE}L = 0$,, that is at $L = n\frac{\lambda^{TE}}{4}$, when $n = 1, 3, 5, \ldots$. This condition takes place when the thickness of the structure is equal to the quarter wavelength or at the following incident angles

$$\theta_{01TE} = \arcsin\sqrt{\mu_{zz}\left(\varepsilon_{yy} - \frac{n^2c^2\pi^2}{4\omega^2L^2\mu_{xx}}\right)},\ n = 1, 3, 5, \ldots;$$

— $\delta^{TE} = 0$ when $\mu_{xx} \to \infty$. Analogously to the case of TM polarized waves, near this characteristic area (ferromagnetic frequency and corresponding external magnetic field), there is a large number of closely located zones of fast change of phase difference. This is due to the large values of k_z^{TE}.

— $\delta^{TE} = \pm\pi$, when$ctgk_z^{TE}L \to \infty$, that is at $L = n\frac{\lambda^{TE}}{2}$, where $n = 0, 1, 2, \ldots$, or at the incident angles

$$\theta_{\pm\pi TE} = \arcsin\sqrt{\mu_{zz}\left(\varepsilon_{yy} - \frac{n^2c^2\pi^2}{\omega^2L^2\mu_{xx}}\right)},\ n = 1, 2, 3, \ldots;$$

— $\delta^{TE} = \pm\pi$, when $\mu_{xx} = \mu_{zz} = 0$;

— at $L = n\frac{\lambda^{TE}}{8}$, $\cot k_z^{TE} L = \pm 1$. Here the upper sign corresponds to $n = 1, 5, 9, \ldots$, and the lower to $n = 3, 7, 11, \ldots$. When this condition takes place, the phase of TE waves can be determined as follows

$$\delta^{TE} = -2\text{arctg}\left[\frac{\pm k_z^{TE}}{k_{zv}\mu_{xx}}\right].$$

4. NUMERICAL SIMULATION

Let us now perform numerical calculations of the above analytical expressions (8)–(9), depending on the magnetic field and frequency.

Since the type and nature of the polarization state are mainly determined by the value of the phase difference, let us first consider the dependence of polarization constants for TE and TM waves versus frequency and magnetic field (Fig. 6, Fig. 7).

Numerical calculations, as before, are performed for the structure where the first layer is the ferrite (brand 1SCH4, $\varepsilon_F = 11.1$, $d_1 = 0.05\,\text{cm}$, $\omega_M = 8.44 \times 10^{10}\,\text{s}^{-1}$, $g = 2$), and the second layer is an n-*InSb* type semiconductor ($\varepsilon_{01} = 17.8$, $d_1 = 0.05\,\text{cm}$, $\omega_P = 2.5 \times 10^{11}\,\text{s}^{-1}$). The thickness of the metamaterial is $L = 5(d_f + d_s)$. We ignore the collision frequency in the semiconductor layers and magnetic damping in the ferrite.

The inserted figures in Fig. 6(b) and Fig. 7(b) correspond to the low frequency range. The shaded areas correspond to the forbidden bands of the metamaterial. As expected, there are a number of characteristic points of unusual behavior, where the phase constants rapidly change from $-\pi$ to π or tend to zero. These features correspond to the mentioned above peculiarities of the effective components of permittivity and permeability of the metamaterial under consideration.

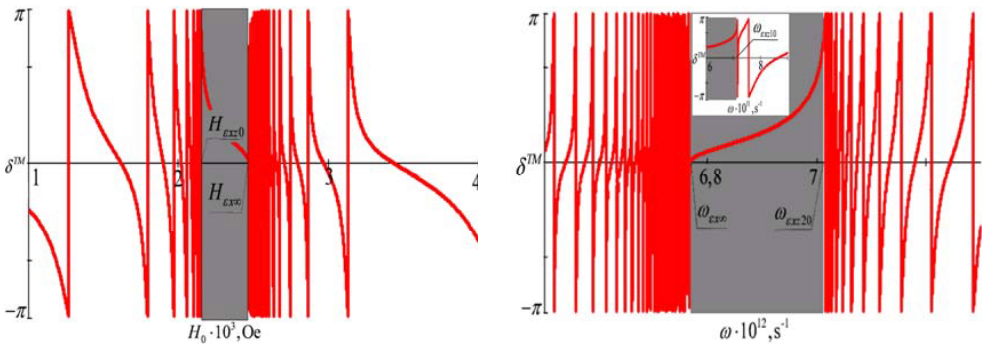

Figure 6. Phase constant for TM-polarization as a function of frequency and external magnetic field.

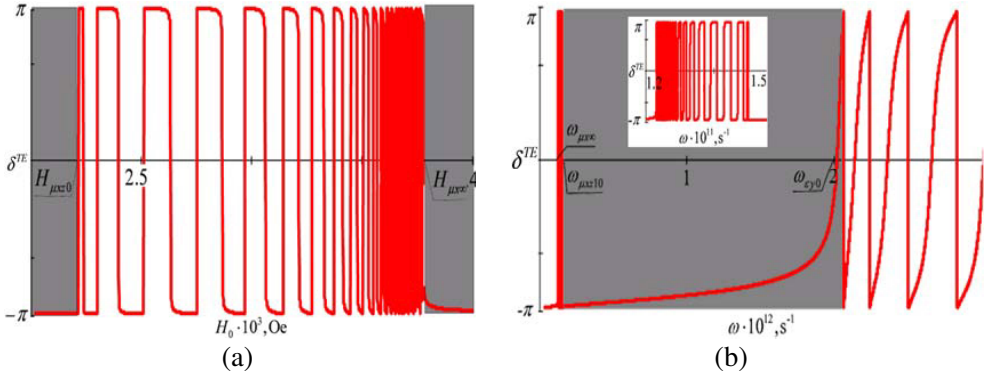

Figure 7. Phase constant for TE-polarization as a function of frequency and external magnetic field.

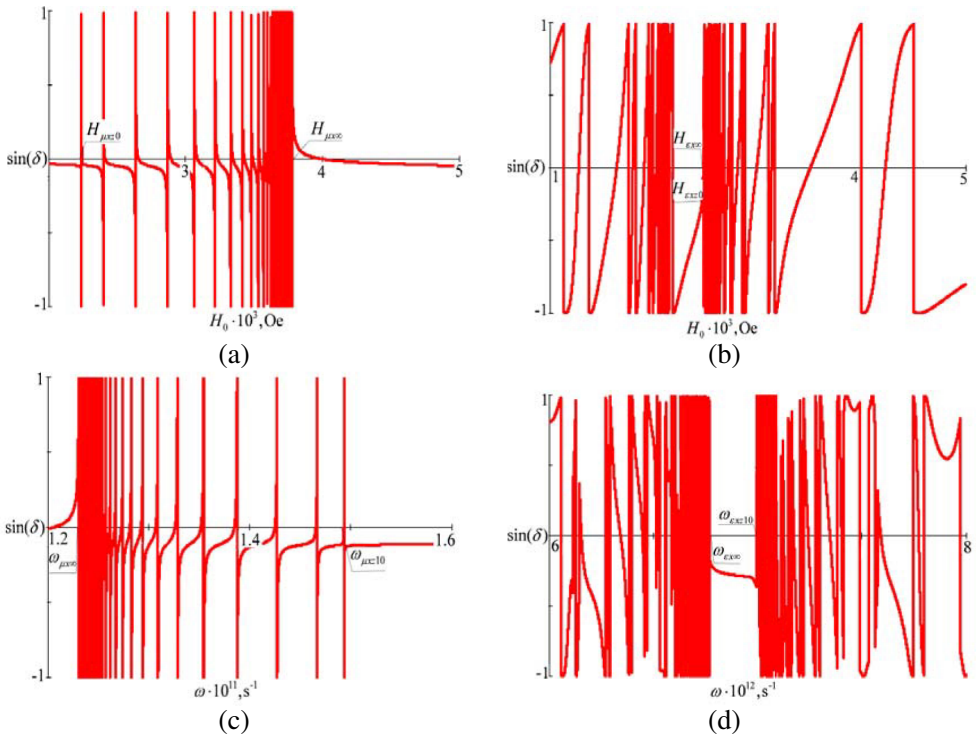

Figure 8. Polarization state (left- and right polarization states) as a function of external magnetic field (a), (b) and frequency (c), (d), $H_0 = 5000\,\text{Oe}$) in different frequency ranges; (a) corresponds to $\omega = 10^{11}\,\text{s}^{-1}$; (b) corresponds to $\omega = 4 \cdot 10^{12}\,\text{s}^{-1}$; left polarization corresponds to $\sin\delta < 0$; right polarization corresponds to $\sin\delta > 0$.

It can be noted that in the vicinity of ferromagnetic resonance frequency $\omega_{\mu x\infty}$ and corresponding magnetic field $H_{\mu x\infty}$, there are a great number of closely located zones of fast change in the polarization state arises of TE-polarized waves. This occurs because at these values of parameters, the Bloch wave number for TE-polarized waves and μ_{xx} tend to infinity (particularly, have large values in real case, when dissipations are taken into account). A similar situation takes place for TM-polarized waves at hybrid frequency $\omega_{\varepsilon x\infty}$ and magnetic field $H_{\varepsilon x\infty}$, where k_z^{TM} and ε_{xx} tend to infinity. At frequencies $\omega_{\varepsilon xz10,\varepsilon xz20}$ and magnetic field $H_{\varepsilon xz0}$ (where $k_z^{TM} \to 0$ and $\varepsilon_{xx} = \varepsilon_{zz} \to 0$), and on the other hand, at frequencies $\omega_{\mu xz0}$, $\omega_{\varepsilon y0}$ and magnetic field $H_{\mu xz0}$ (where $k_z^{TE} \to 0$, $k_z^{TM} \to 0$, and $\mu_{xx} = \mu_{zz} \to 0$), the polarization constants for TM- and TE-polarizations become zero. Other features observed in the dependences correspond to the cases when the optical thickness of the structure for particular wave is equal to half wavelength, quarter wavelength or eighth wavelength (see the equations above).

Another interesting and important characteristic to be considered is the direction of polarization ellipse rotation and more specific is the areas in which we have left ($\sin\delta < 0$) or right ($\sin\delta > 0$) polarized electromagnetic wave, in the absence of dissipation (Fig. 8).

It can be seen that there are a number of bands in which the electromagnetic wave has left and right polarization states, due to the specific features of the considered structure. As the general features are similar to the considered above, let us only mention here, as earlier, of great interest representing the frequencies in the vicinity of the hybrid resonance frequency and the frequency of ferromagnetic resonance, where there are a number of closely located zones, where a small change in a frequency or magnetic field results in the changes of direction of polarization ellipse bypass. So, by varying the physical and geometrical parameters of the metamaterials, it is possible to effectively control the polarization state.

The view of polarization ellipse versus different values of the external magnetic field is presented in Fig. 9(a) and as a function of metamaterial thickness at Fig. 9(b) ($\omega = 4 \cdot 10^{12}\,\text{s}^{-1}$, $\theta = \pi/6$).

Thus, we can summarize that due to the anisotropy and specific features of the considered

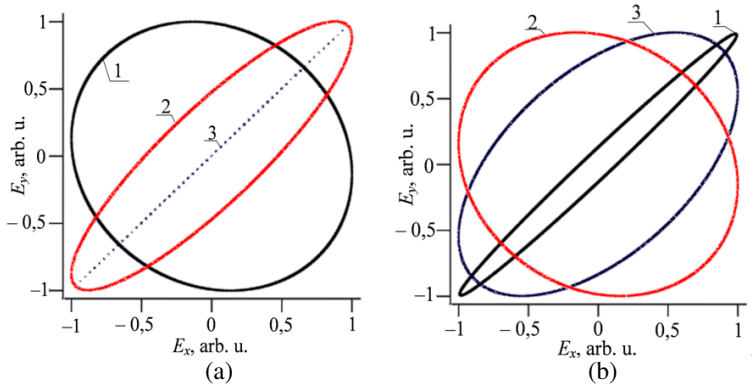

Figure 9. Polarization ellipse for different external magnetic field magnitudes and thicknesses of the metamaterial without dissipations; at Fig. 9(a): 1 — $H_0 = 1300\,Oe$; 2 — $H_0 = 1500\,Oe$; 3 — $H_0 = 1950\,Oe (N = 5)$; at Fig. 9(b): 1 — $N = 5$; 2 — $N = 10$; 3 — $N = 15$ ($H_0 = 2000$ Oe).

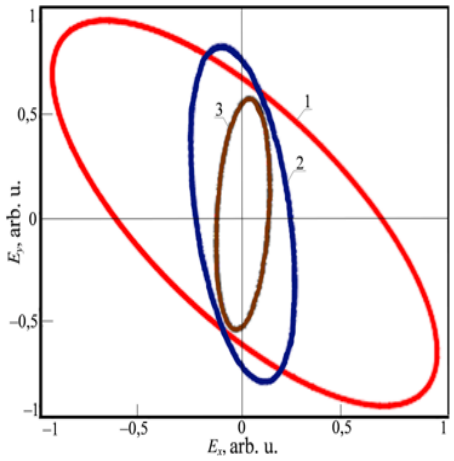

Figure 10. Polarization ellipse when the dissipation processes in the layers are taken into account; 1 — $\nu = 0$, $\omega_r = 0$; 2 — $\nu \approx 10^{10}\,\mathrm{s}^{-1}$, $\omega_r \approx 10^8\,\mathrm{s}^{-1}$; 3 — $\nu \approx 5 \cdot 10^{10}\,\mathrm{s}^{-1}$, $\omega_r \approx 10^8\,\mathrm{s}^{-1}$.

subwavelength metamaterial, effective control of the polarization state by mean of frequency, external magnetic field, thicknesses of the layers and the entire metamaterial, physical parameters of materials, composed the metamaterial is possible. Namely we can control the value of polarization ellipse axes, axis inclination angle, as well as the left and right polarization states.

Moreover, it should also be noted that as can be seen, in some areas the effective linear-to-linear and linear-to-elliptic polarization transformation is possible.

Finally, let us consider the effect of dissipations, namely the collision frequency in the semiconductor layer and damping in the ferrite layer, on the polarization ellipse parameters (Fig. 10).

As already mentioned above, when the losses in the layers are taken into account, there are no abrupt changes at the effective permittivity and permeability dependences, and consequently, the phase differences dependences, and the corresponding curves are smoothed. This is because the components of the permittivity and permeability of the considered metamaterial, and consequently, the Bloch wave numbers become complex. With the reduction of the collision frequency, the effect of anisotropy of the structure becomes more dominant, and more abrupt changes at the corresponding dependences occur (Fig. 10).

Let us note that unlike the case, where there are no losses in the layers (curve 1), when we take into account dissipation processes, the value of the polarization ellipse axis decreases, the inclination angle changes, and the ellipse shape transformation takes place.

5. CONCLUSIONS

Thus, in this paper, it has been shown that it is possible to effectively control the polarization state of the reflected electromagnetic wave (namely phase difference, polarization rotation angle, to name a few) by means of altering magnetic field, thicknesses of the layers and physical parameters of materials, which form the structure under consideration. In the vicinity of ferromagnetic resonance frequency and corresponding value of external magnetic field, the optical width of the ferrite layers tends to infinity, which leads to the formation of numerous narrow transmission bands, and bands of fast polarization state change. The same situation takes place close to the hybrid frequency and corresponding magnetic filed, where the width of the semiconductor layer tends to infinity.

The results of our investigations can be used in the implementation of the variety of microwave and optical devices, for the analysis of various kinds of PCs, for exact measurement of an external magnetic field, etc. Our work opens new opportunities for creating high performance photonic devices and enables emergent metamaterial functionalities for applications in the technologically difficult terahertz frequency regime. Thin films on a metal substrate have many practical uses. They are employed, for example, to protect metallic mirrors and to increase their reflectivity. They may also be used to reduce the reflectivity of a metal surface, in optics, electronics, and photovoltaic cell, to name a few [1–5].

REFERENCES

1. Grady, N. K., J. E. Heyes, D. R. Chowdhury, Y. Zeng, M. T. Reiten, A. K. Azad, A. J. Taylor, D. A. R. Dalvit, and H.-T. Chen, "Terahertz metamaterials for linear polarization conversion and anomalous refraction," *Science*, Vol. 340, No. 6138, 1304–1307, 2013.
2. Tuz, V., M. Vidil, and S. Prosvirnin, "Polarization transformations by a magneto-photonic layered structure in the vicinity of a ferromagnetic resonance," *J. Opt.*, Vol. 12, 095102, 2010.
3. Born, M. and E. Wolf, *Principles of Optics*, Pergamon Press, Oxford, 1965.
4. Hallam, B. T., C. R. Lawrence, I. R. Hooper, and J. R. Sambles, "Broad-band polarization conversion from a finite periodic structure in the microwave regime," *Applied Physics Letters*, Vol. 84, No. 6, 849–851, 2004.
5. Tuz, V. and V. Kazanskiy, "Periodicity defect influence on the electromagnetic properties of a sequence with bi-isotropic layers," *Progress In Electromagnetics Research B*, Vol. 7, 299–307, 2008.
6. Bass, F. G. and A. A. Bulgakov, *Kinetic and Electrodynamic Phenomena in Classical and Quantum Semiconductor Superlattices*, Nova Science, NY, 1997.
7. Bulgakov, A. A., A. A. Girich, M. K. Khodzitsky, O. V. Shramkova, and S. I. Tarapov, "Transmission of electromagnetic waves in a magnetic fine-stratified structure," *J.Opt. Soc.Am.B*, Vol. 26, No. 12, B156–B160, December 2009.
8. Polevoy, S., S. Prosvirnin, S. Tarapov, and V. Tuz, "Resonant features of planar Faraday metamaterial with high structural symmetry. Study of properties of a 4-fold array of planar chiral rosettes placed on a ferrite substrate," *Eur. Phys. J. Apll. Phys.*, Vol. 61, No. 3, 30501 (7 pages), 2013.
9. Passilly, N., P. Karvinen, K. Ventola, P. Laakkonen, J. Turunen, and J. Tervo, "Polarization conversion by dielectric subwavelength gratings in conical mounting," *Journal of the European Optical Society — Rapid Publications*, Vol. 3, 08009 (7 pages), 2008.
10. Cong, L., W. Cao, Zh. Tian, J. Gu, J. Han, and W. Zhang, "Manipulating polarization states of terahertz radiation using metamaterials," *New Journal of Physics*, Vol. 14, 115013 (11 pages), 2012.
11. Poddubny, A., I. Iorshm, P. Belov, and Y. Kivshar, "Hyperbolic metamaterials," *Nature Photonics*, Vol. 7, 948–957, 2013.
12. Fang, W. and S. Xu, "Realization of complete polarization conversion using periodic structure composed of left-handed materials," *Microwave and Optical Technology Letters*, Vol. 49, No. 11, 2862–2864, 2007.

13. Zhang, Y., Y. Jiang, W. Xue, and S. He, "A broad-angle polarization splitters based on a simple dielectric periodic structure," *Opt. express*, Vol. 15 (22), 14363-8, 2007.
14. Bai, B., K. Ventola, J. Tervo, and Y. Zhang, "Determination of the eigenpolarizations in arbitrary diffraction orders of planar periodic structures under arbitrary incidence," *Phys. Rev. A*, Vol. 85, 053808 (8 pages), 2012.
15. Ye, Y., X. Li, F. Zhuang, and S.-W. Chang, "Homogeneous circular polarizers using a bilayered chiral metamaterial," *Phys. Lett*, Vol. 99, 031111 (3 pages), 2011.
16. Semchenko, I.V., S. A. Khakhomov, and A. L. Samofalov, "Polarization plane rotation of electromagnetic waves by the artificial periodic structure with one-turn helical elements," *Electromagnetics*, Vol. 26, 219–233, 2006.
17. Chen, H. T., J. F. O'Hara, A. J. Taylor, R. D. Averitt, C. Highstrete, M. Lee, and W. J. Padilla, "Complementary planar terahertz metamaterials," *Opt. Express*, Vol. 15, 1084–1095, 2007.
18. Tuz, V. R., O. D. Batrakov, and Y. Zheng, "Gyrotropic-nihility in ferrite-semiconductor composite faraday geometry," *Progress In Electromagnetics Research B*, Vol. 41, 397–417, 2012.
19. Baibak, V. V., I. V. Fedorin, and A. A. Bulgakov, "Polarization conversion by a 1-d photonic crystal located on isotropic and anisotropic substrates," *Telecommunications and Radio Engineering*, Vol. 73, No 6, 555–567, 2014.
20. Bulgakov, A. A. and I. V. Fedorin, "Ellipsoidal properties of the reflection factors from a thin-layer periodic semiconductor-dielectric structure in a magnetic field," *Telecommunications and Radio Engineering*, Vol. 71, No. 13, 1213–1227, 2012.
21. Jung, H., C. In, H. Choi, and H. Lee, "Anisotropy modeling of terahertz metamaterials: polarization dependent resonance manipulation by meta-atom cluster," *Scientific Reports*, Vol. 4, No. 5217, (7 pages), 2014.
22. Mousavi, S. A., E. Plum, J. Shi, and N. I. Zheludev, "Coherent control of optical polarization effects in metamaterials," *Sci Rep.*, Vol. 10, No. 5, 8977, 2015.
23. Bulgakov, A. A. and I. V. Fedorin, "Electrodynamic properties of a thin-film periodic structure in an external magnetic field," *Technical Physics*, Vol. 56, No. 4, 510–514, 2011.
24. Baibak, V. V., I. V. Fedorin, and A. A. Bulgakov, "Surface electromagnetic waves in finite semiconductor-dielectric periodic structure in an external magnetic field," *Progress In Electromagnetics Research M*, Vol. 32, 229–244, 2013.
25. Shramkova, O. V., "Transmission spectra in ferrite-semiconductor periodic structure," *Progress In Electromagnetic Research M*, Vol. 7, 71–85, 2009.
26. Landau, L. D. and E. M. Lifshits, *Electrodynamics of Continuous Media*, 2nd Edition, Pergamon Press, Oxford, England, 1984.